Journal of Sound and Vibration 329 (2010) 3319–3324

Contents lists available at ScienceDirect

Journal of Sound and Vibration

journal homepage: www.elsevier.com/locate/jsvi

Transition from progressive to quasi-standing waves behavior of the radiation force of acoustic waves—Example of a high-order Bessel beam on a rigid sphere

F.G. Mitri *

Mayo Clinic, College of Medicine, Department of Physiology and Biomedical Engineering, Ultrasound Research Laboratory, 200 First Street SW, Rochester, MN 55905, USA

ARTICLE INFO

Article history:
Received 11 December 2009
Accepted 24 February 2010
Handling Editor: Y. Auregan
Available online 16 March 2010

ABSTRACT

Prior computations have predicted the time-averaged acoustic radiation force on fluid spheres in water when illuminated by an acoustic high-order Bessel beam (HOBB) of quasi-standing waves. These computations are extended to the case of a rigid sphere in water which perfectly mimics a fluid sphere in air. Numerical results for the radiation force function of a HOBB quasi-standing wave tweezers are obtained for beams of zero, first and second order, and discussed with particular emphasis on the amplitude ratio describing the transition from progressive waves to quasi-standing waves behavior. This investigation may be helpful in the development of acoustic tweezers and methods for manipulating objects in reduced gravity environments and space related applications.

1. Introduction

The analysis of the radiation force exerted on a particle in either an electromagnetic or acoustic field has attracted many researchers in the field of laser and acoustical trapping [1–6]. Laser-trapping has been widely used for the measurement of pico-Newton order forces that are associated with interactions of particles in micrometer or nanometer regions [7]. Similarly, acoustical tweezers have found interesting applications in particle manipulation and entrapment [8–10]. Sound carries energy and momentum, and hence the radiation force of acoustical tweezers is produced by the exchange of momentum and energy between the wave and the particle placed along its path.

The majority of acoustical traps (or tweezers) use a pair of coaxial transducers emitting counterpropagating acoustical waves. Usually, the beams' type corresponds to focused Gaussian profiles [9]. However, Gaussian beams suffer from the natural diffractive spreading as explained by the Huygens–Fresnel principle. In addition, Gaussian beams are only useful for particle trapping when the index of refraction inside the particle exceeds the ambient index of refraction [6]. This effect led researchers to use doughnut-shaped laser beams (or "hollow" beams) for particle manipulation and entrapment [11–13].

One type of "hollow" beams has a Bessel function of the first kind of order m usually denoted by J_m. Such beams are therefore termed "Bessel beams". Bessel beams are localized in transverse direction [14] and have potential applications in various areas of research including medical acoustical imaging [15,16], particle manipulation with optical tweezers [17–20] and promising relevance in designing acoustical tweezers. In the field of acoustics, recent theoretical research has

* Present address: Los Alamos National Laboratory, MPA-11, Sensors & Electrochemical Devices, Acoustics & Sensors Technology Team, MS D429, Los Alamos, NM 87545, USA.
E-mail address: mitri@lanl.gov

0022-460X/$ - see front matter © 2010 Elsevier Ltd. All rights reserved.
doi:10.1016/j.jsv.2010.02.025

been focused on studying the acoustic radiation force of *zero-order* (m=0) Bessel beam tweezers on an elastic spherical particle [21,22]. In those studies, it has been shown that the direction of the force depends on the axial position in the acoustic standing or quasi-standing wave field, as well as the mechanical properties of the sphere. Furthermore, earlier investigations using zero-order Bessel acoustic beams of progressive waves [23,24] have predicted a negative force on fluid and elastic spheres and spherical shells [25,26].

It is particularly important to note that the fundamental zero-order Bessel beam has an amplitude maximum at the origin, whereas a high-order Bessel beam (HOBB) of order m possesses an axial phase singularity at the transverse origin where the amplitude vanishes as expected from the mathematical descriptive nature of the high-order Bessel function of the first kind $J_{m>0}$ [27]. For this reason, such beams are termed "hollow beams".

One may therefore ask if such hollow beams exert a radiation force on an object placed along their path, and under which circumstances this effect occurs. Recent theoretical investigations [28–32] have confirmed the existence of the radiation force on a rigid sphere [28,31,32], a spherical air bubble and fluid spheres of various densities immersed in non-viscous water [29,30]. An especially noteworthy result illustrated in [29,30] is the lack of a specific vibrational resonance mode contribution to the radiation force determined by appropriate selection of the HOBB parameters. The present investigation extends the prior work [29] to the case of a rigid sphere in non-viscous water which perfectly mimics a fluid sphere in air. The rigid sphere example is of particular importance for various applications in particle manipulation and trapping using acoustical waves since it perfectly models the levitation of fluid drops in air [33]. In practical applications, "perfect" standing waves may be difficult to achieve because of the acoustic reflection on the tweezers' boundaries. In fact, the resulting acoustic field is a *quasi-standing* wave-field characterized by its specific wave amplitudes Φ_0 and Φ_1 that create the beam. In this paper, the radiation force function, which is the radiation force per unit energy density and unit cross-sectional surface, is numerically evaluated for a rigid immovable sphere. The acoustic scattering of the beam composed of quasi-standing waves, which is characterized by its half-cone angle β of the wavenumber components, the waves' amplitudes Φ_0 and Φ_1, and the order m of the HOBB, is used to evaluate the radiation force function. Numerical examples are provided and discussed with particular emphasis on the waves' amplitude ratio describing the transition from progressive to quasi-standing waves behavior.

2. Computation of the axial radiation force of a high-order Bessel beam on a rigid sphere

Relevant results for the computation of the force are summarized here. The axial radiation force in a quasi-standing HOBB wave-field on a sphere of radius a is related to a dimensionless radiation force function $Y_{J_m,qst}$ by [29]

$$\langle F_z \rangle_{J_m,qst} = Y_{J_m,qst} S_c E, \tag{1}$$

where $E=\rho k^2|\Phi_0|^2/2$ is the characteristic energy density, ρ is the mass density of the surrounding fluid, $k=\omega/c=2\pi/\lambda$, is defined as the wavenumber of the incident HOBB, ω is the angular frequency, c is the speed of sound in the fluid medium, λ being the wavelength of the acoustic radiation making up the HOBB, Φ_0 is the amplitude of the wave propagating along the positive direction of the z-axis, and $S_c=\pi a^2$ is the cross-sectional area. The dimensionless factor $Y_{J_m,qst}$ is defined as the radiation force function for a HOBB of quasi-standing waves, and is expressed by [29]

$$Y_{J_m,qst} = \frac{8}{(ka)^2}\sum_{n=m}^{\infty}\left\{\begin{array}{l}\left[\begin{array}{l}(-1)^{(n+1)}\left(\dfrac{|\Phi_1|}{|\Phi_0|}\right)[\beta_n(1+2\alpha_{n+1})-\beta_{n+1}(1+2\alpha_n)]\sin(2k_z h)\\ \quad -\left(\dfrac{|\Phi_0|^2-|\Phi_1|^2}{2|\Phi_0|^2}\right)[\alpha_n+\alpha_{n+1}+2(\alpha_n\alpha_{n+1}+\beta_n\beta_{n+1})]\end{array}\right]\\ \times\dfrac{(n-m+1)!}{(n+m)!}P_n^m(\cos\beta)P_{n+1}^m(\cos\beta)\end{array}\right\}, \tag{2}$$

where $P_n^m(\cdot)$ are the associated Legendre functions of the first kind, $k_z=k\cos\beta$ where β is the half-cone angle formed by the wavenumber k relative to the axis of wave propagation (z-axis), h is the distance in the z-direction from the center of the sphere to the nearest velocity potential antinode, Φ_1 is the amplitude of the wave propagating along the negative direction of the z-axis and is assumed to be smaller than Φ_0 and α_n and β_n are the real and imaginary part of the scattering coefficients $A_n=(\alpha_n+i\beta_n)$. These coefficients are known for a rigid immovable (fixed) sphere [34] to be

$$A_n = -\frac{j_n'(ka)}{h_n^{(1)'}(ka)}, \tag{3}$$

where $j_n(\cdot)$ is the spherical Bessel function of the first kind of order n, $h_n^{(1)}(\cdot)$ denotes the spherical Hankel function of the first kind and the primes denote their derivatives with respect to the argument.

3. Numerical results and discussion

Numerical values of $Y_{J_m,qst}$ as given by Eq. (2) are evaluated for a rigid immovable sphere immersed in non-viscous water. It is appropriate to investigate the rigid case since the sphere elicits no elastic vibration and the scattering is well known. This example is of some fundamental importance in fluid dynamics applications because it simulates the

interaction of acoustical axisymmetric HOBBs in a reduced gravity environment with a levitated liquid drop in air while maintaining its spherical shape. Since the drop is usually about 813 times denser than air and the acoustic impedances of liquid and air are mismatched, liquid drops in air are adequately approximated as perfectly rigid objects, and the time-averaged radiation force is not sensitive to the density or sound speed of the drop [33]. In this example, the surrounding fluid medium has a density of $\rho=1000\,\mathrm{kg/m^3}$, and a speed of sound of $c=1500\,\mathrm{m/s}$. Realizing the large number of variables in Eq. (2), no attempt is made here to study the variations of each of them. Therefore, the attention is focused on a typical example model in which the half-cone angle has a fixed value, i.e. $\beta=65^\circ$. The $Y_{J_m,qst}$ curves are subsequently evaluated for a HOBB of zero, first and second order, respectively, with particular emphasis on three amplitude ratios $|\Phi_1|/|\Phi_0|$ of the quasi-standing wave field. The ratio $|\Phi_1|/|\Phi_0|=0$ corresponds to a pure progressive wave [28,30], $|\Phi_1|/|\Phi_0|=1$ corresponds to a pure standing wave [32], and $|\Phi_1|/|\Phi_0|=0.5$ is for a typical quasi-standing wave field. Moreover, the curves are plotted in the bandwidth $0\leq ka\leq 10$. For the ease of the computational evaluation of Eq. (2), the parameter h is chosen to be dependent on the wavenumber k (or frequency) and the half-cone angle β such that $h=\pi/(4k\cos\beta)$; the sphere is therefore assumed to be located at the intermediate location between a pressure node and a pressure antinode in the quasi-standing wave field [21]. Accurate computation of the spherical Bessel, Neumann, and Hankel functions is achieved using modified versions of Matlab (Math Works, Natick, MA) specialized math functions "besselj," "bessely," and "besselh." The convergence of calculations are systematically checked in a simple trail and error manner, by decreasing the tolerance in the accuracy of the acceptable solutions (i.e. indirectly increasing the number of iterations) while looking for steadiness or stability in the numerical value of the calculated radiation force functions. Calculations of the series given in Eq. (2) are evaluated in the bandwidth $0\leq ka\leq 10$. The computational increment of $\Delta ka=10^{-2}$ is used. Since the sphere is rigid immovable and exhibits no resonances, decreasing Δka has no effect on the radiation force function curves.

Fig. 1 shows the comparison between the zero-, first-, and second-order Bessel beam radiation force function $Y_{J_m,qst}$ curves as a function of ka with the amplitude ratio $|\Phi_1|/|\Phi_0|=0$ and $\beta=65^\circ$. The curves correspond to a HOBB of pure progressive waves. For the zero-order ($m=0$) Bessel beam, the form of Eq. (2) reduces to Eq. (10b) in [25]. One particularly notices the increase in the radiation force function values around $ka\approx 1.65$. This amplitude peak is found to be correlated with conditions giving acoustic scattering enhancement into the backwards hemisphere [25,26]. The dashed curve in Fig. 1 corresponds to a first-order ($m=1$) Bessel beam. It shows that the radiation force function exhibits negative values around $ka\approx 1.738$ that can be associated with a reduction of the acoustic scattering into the backwards hemisphere [31]. In the axial direction, the forward acoustic scattering ($\theta=0$) and backscattering ($\theta=\pi$) vanish [35–37]. This phenomenon was previously anticipated from experimental observations related to the design and the evaluation of an acoustical helicoidal transducer having an azimuthal dependence on the phase [38]. The dot-dashed curve in Fig. 1 shows the $Y_{J_m,qst}$ curve for a second-order ($m=2$) Bessel beam. One notices the similar behavior of the curve's variations as compared with the dashed curve of a Bessel beam of first-order; however, the amplitude values are reduced. As ka increases ($\sim ka>5$), the radiation force function $Y_{J_m,qst}$ curves converge to comparable amplitude values.

Fig. 2 shows the comparison between the zero-, first-, and second-order Bessel beam radiation force function $Y_{J_m,qst}$ curves as a function of ka with the amplitude ratio $|\Phi_1|/|\Phi_0|=0.5$ and $\beta=65^\circ$. The curves correspond to a HOBB of typical quasi-standing waves. For the zero-order ($m=0$) Bessel beam, the form of Eq. (2) reduces to Eq. (18) in [21]. For the first- and second-order Bessel beams, $Y_{J_m,qst}$ curves exhibit positive as well as negative values. The force is directed towards a pressure node when $Y_{J_m,qst}>0$ and is directed towards a pressure antinode if $Y_{J_m,qst}<0$. The exact equilibrium position can

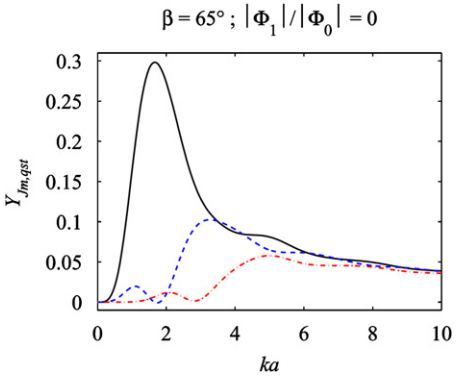

Fig. 1. (Color online) The plots where $Y_{J_m,qst}$ curves are computed by Eq. (11) for a rigid immovable sphere immersed in water and placed in a zero- (solid line —), first- (dashed line – – –), and second-order (dashed-dotted line – · – · –) Bessel beam, respectively. The curves are plotted as a function of ka with the amplitude ratio $|\Phi_1|/|\Phi_0|=0$ and $\beta=65^\circ$. The curves correspond to beams of pure progressive waves. For $m=0$, one particularly notices the increase in the radiation force function values around $ka\approx 1.65$. The dashed curve in Fig. 1 corresponds to a first-order ($m=1$) Bessel beam. It shows that the radiation force function exhibits a minimum at $(ka,Y_{J_m,qst})=(1.738,-8.0857\times 10^{-4})$. The dot-dashed curve shows the $Y_{J_m,qst}$ curve for a second-order ($m=2$) Bessel beam. One notices the similar behavior of the curve's variations as compared with the dashed curve of a Bessel beam of first-order; however, the amplitude values are reduced. As ka increases ($\sim ka>5$), the radiation force function $Y_{J_m,qst}$ curves converge to comparable amplitude values.

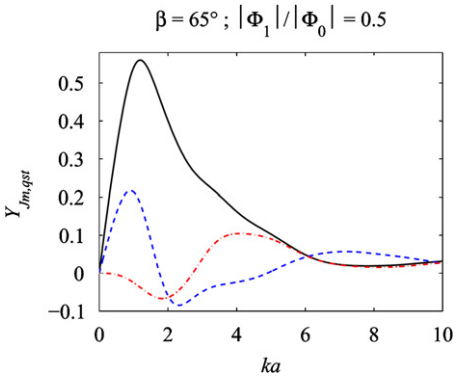

Fig. 2. (Color online) The same as in Fig. 1, but the curves are plotted for the amplitude ratio $|\Phi_1|/|\Phi_0| = 0.5$. The curves correspond to typical HOBB quasi-standing waves. The dashed and dot-dashed curves corresponding to the first- and second-order Bessel beams, respectively, exhibit positive as well as negative values. The force is directed towards a pressure node when $Y_{J_m,qst} > 0$ and is directed toward a pressure antinode if $Y_{J_m,qst} < 0$.

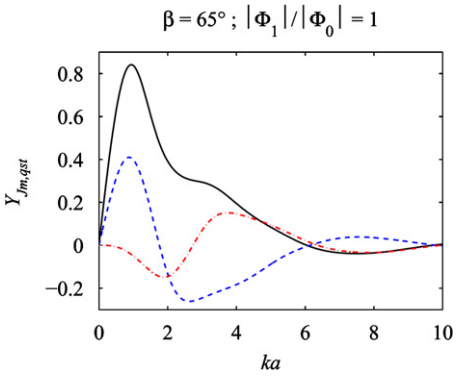

Fig. 3. (Color online) The same as in Fig. 1, but the curves are plotted for the amplitude ratio $|\Phi_1|/|\Phi_0| = 1$. The curves correspond to equi-amplitude (pure) standing waves. One particularly notices the similar behavior of the curve's variations as compared with Fig. 2 for quasi-standing HOBBs. However, the absolute amplitude values of the $Y_{J_m,qst}$ curves are amplified for HOBB standing waves.

be predicted from the expression of $Y_{J_m,qst}$ in Eq. (2) for a particular frequency. The particle immobilization at the equilibrium position may be used for advantage to predict some properties of the sphere as well as the HOBB quasi-standing wave field.

Fig. 3 shows the comparison between the zero-, first-, and second-order Bessel beam radiation force function $Y_{J_m,qst}$ curves as a function of ka with the amplitude ratio $|\Phi_1|/|\Phi_0| = 1$ and β=65°. The curves correspond to beams of pure standing waves. For the zero-order (m=0) Bessel beam, the form of Eq. (2) reduces to Eq. (15) in [21]. One particularly notices the similar behavior of the curve's variations as compared with Fig. 2 for quasi-standing HOBBs. Nevertheless, the absolute amplitude values of the $Y_{J_m,qst}$ curves are amplified for HOBB standing waves. This result can be expected by further mathematical analysis of Eq. (2); this equation shows that in a HOBB quasi-standing wave, the force is the combination of two forces, one induced by a standing wave, and the other by a progressive wave. As the ratio $|\Phi_1|/|\Phi_0|$ in Eq. (2) increases from 0 to 1, the factor $(|\Phi_0|^2-|\Phi_1|^2)/(2|\Phi_0|^2)$ decreases from 1/2 to 0. As a result, absolute values of $Y_{J_m,qst}$ curves increase and reach the limit of pure standing waves.

The particular analysis of Eq. (2) for which the order m and the half-cone angle β both equal zero, shows that $Y_{J_m,qst}$ reduces to the expression of the radiation force function of plane quasi-standing waves Y_{qst} as given in [39]. This result is somehow expected since the product of the Legendre functions $P_n^0(1)P_{n+1}^0(1)$ equals unity. In a recent work using the far-field method (see the discussion in Section 3 in [32]), an expression of the radiation force resulting from a so called "superposition of a plane progressive wave and a standing wave", which actually corresponds to a plane quasi-standing wave, is obtained [40]. That expression may at first appear to be a different form of Y_{qst} given previously by a far-field method (i.e. Eq. (19) in [33]) or by a near-field method (i.e. Eq. (26) in [39], [41]). Rewriting Eq. (1) in [40] (which represents the incident pressure field on the sphere) in a spherical coordinates system as

$$p(z) = p_0 \sum_{n=0}^{\infty} \left[\varepsilon e^{ikh} + \eta(e^{ikh} + (-1)^n e^{-ikh})\right] i^n (2n+1) j_n(kr) P_n(\cos\theta), \tag{4}$$

where $p_0=\rho kc\Phi_0$, the parameters ε and η are amplitude constants determined by $(\varepsilon+\eta)=1$ [40], and expressing the total (incident+scattered) pressure field as

$$p_t(z)=p_0\sum_{n=0}^{\infty}[\varepsilon e^{ikh}+\eta(e^{ikh}+(-1)^n e^{-ikh})]i^n(2n+1)[j_n(kr)+A_n h_n^{(1)}(kr)]P_n(\cos\theta), \tag{5}$$

the resultant *axial* time-averaged acoustic radiation force in the plane wave limit is obtained after substituting Eq. (5) into Eq. (14) in [33], and manipulating the result to give,

$$\langle F_z\rangle_{qst}=Y_{qst}S_cE, \tag{6}$$

where

$$Y_{qst}=\frac{8}{(ka)^2}\sum_{n=0}^{\infty}(n+1)\left\{\left[\begin{array}{l}(-1)^{(n+1)}(\eta^2+\varepsilon\eta)[\beta_n(1+2\alpha_{n+1})-\beta_{n+1}(1+2\alpha_n)]\sin(2kh)\\ -\left(\dfrac{\varepsilon^2+2\varepsilon\eta}{2}\right)[\alpha_n+\alpha_{n+1}+2(\alpha_n\alpha_{n+1}+\beta_n\beta_{n+1})]\end{array}\right]\right\}. \tag{7}$$

It is obvious that Eq. (7) equals Eq. (19) in [33] and Eq. (26) in [39] in the limits,

$$\left\{\begin{array}{l}\left(\dfrac{|\Phi_1|}{|\Phi_0|}\right)=(\eta^2+\varepsilon\eta),\\ \left(1-\dfrac{|\Phi_1|^2}{|\Phi_0|^2}\right)=(\varepsilon^2+2\varepsilon\eta).\end{array}\right. \tag{8}$$

Therefore, the expression for the force given in [40] is commensurate with the same results given in [33] and [39] with no particular advantage.

4. Conclusion

These calculations predict the axial radiation force on a rigid sphere illuminated by an axisymmetric HOBB of quasi-standing waves. It is appropriate to investigate the rigid case since the sphere elicits no elastic vibration and the scattering is well known. Typical numerical examples for the radiation force function $Y_{J_m,qst}$ are obtained for beams of zero-, first- and second-order, with particular emphasis on the amplitude ratio describing the transition from progressive waves to quasi-standing waves behavior. These examples simulate the interaction of HOBB in a reduced gravity environment with a levitated liquid drop in air and maintaining its spherical shape. They may be used to advantage in various areas in fluid dynamics application using HOBBs for particle manipulation and entrapment.

References

[1] F.E. Borgnis, Acoustic radiation pressure of plane compressional waves, *Reviews of Modern Physics* 25 (1953) 653–664.
[2] R. Klima, V.A. Petrzilka, On the radiation pressure of electromagnetic wave packets in nondispersive fluid dielectrics, *Annals of Physics* 92 (1975) 395–405.
[3] H. Metcalf, P. Vanderstraten, Cooling and trapping of neutral atoms, *Physics Reports* 244 (1994) 204–286.
[4] A.A. Doinikov, Theory of acoustic radiation pressure for actual fluids, *Physical Review E* 54 (1996) 6297–6303.
[5] A.A. Doinikov, Acoustic radiation forces: classical theory and recent advances, *Recent Research and Development in Acoustics* 1 (2003) 39–67.
[6] C.-L. Zhao, L.-G. Wang, X.-H. Lu, Radiation forces on a dielectric sphere produced by highly focused hollow Gaussian beams, *Physics Letters A* 363 (2007) 502–506.
[7] A. Ashkin, Optical trapping and manipulation of neutral particles using lasers, *Proceedings of the National Academy of Sciences of the United States of America* 94 (1997) 4853–4860.
[8] H.M. Hertz, Standing-wave acoustic trap for nonintrusive positioning of microparticles, *Journal of Applied Physics* 78 (1995) 4845–4849.
[9] J. Wu, Acoustical tweezers, *Journal of the Acoustical Society of America* 89 (1991) 2140–2143.
[10] E.H. Brandt, Acoustic physics—suspended by sound, *Nature* 413 (2001) 474–475.
[11] B.T. Unger, P.L. Marston, Optical levitation of bubbles in water by the radiation pressure of a laser beam: an acoustically quiet levitator, *Journal of the Acoustical Society of America* 83 (1988) 970–975.
[12] G. Zhou, X. Chu, J. Zheng, Investigation in hollow Gaussian beam from vectorial structure, *Optics Communications* 281 (2008) 5653–5658.
[13] Y. Cai, F. Wang, Partially coherent anomalous hollow beam and its paraxial propagation, *Physics Letters A* 372 (2008) 4654–4660.
[14] C. Lopez-Mariscal, J.C. Gutierrez-Vega, The generation of nondiffracting beams using inexpensive computer-generated holograms, *American Journal of Physics* 75 (2007) 36–42.
[15] J.Y. Lu, T.K. Song, R.R. Kinnick, J.F. Greenleaf, In-vitro and in-vivo real-time imaging with ultrasonic limited diffraction beams, *IEEE Transactions on Medical Imaging* 12 (1993) 819–829.
[16] J.Y. Lu, Designing limited diffraction beams, *IEEE Transactions on Ultrasonics Ferroelectrics and Frequency Control* 44 (1997) 181–193.
[17] J. Arlt, K. Dholakia, Generation of high-order Bessel beams by use of an axicon, *Optics Communications* 177 (2000) 297–301.
[18] J. Arlt, T. Hitomi, K. Dholakia, Atom guiding along Laguerre–Gaussian and Bessel light beams, *Applied Physics B—Lasers and Optics* 71 (2000) 549–554.
[19] J. Fan, E. Parra, I. Alexeev, K.Y. Kim, H.M. Milchberg, L.Y. Margolin, L.N. Pyatnitskii, Tubular plasma generation with a high-power hollow Bessel, *Physical Review E* 62 (2000) R7603–R7606.
[20] V. Garces-Chavez, D. Roskey, M.D. Summers, H. Melville, D. McGloin, E.M. Wright, K. Dholakia, Optical levitation in a Bessel light beam, *Applied Physics Letters* 85 (2004) 4001–4003.
[21] F.G. Mitri, Acoustic radiation force on a sphere in standing and quasi-standing zero-order Bessel beam tweezers, *Annals of Physics* 323 (2008) 1604–1620.
[22] F.G. Mitri, Z.E.A. Fellah, Theory of the acoustic radiation force exerted on a sphere by a standing and quasi-standing zero-order Bessel beam tweezers of variable half-cone angles, *IEEE Transactions on Ultrasonics Ferroelectrics and Frequency Control* 55 (2008) 2469–2478.

[23] P.L. Marston, Scattering of a Bessel beam by a sphere, *Journal of the Acoustical Society of America* 121 (2007) 753–758.
[24] P.L. Marston, Acoustic beam scattering and excitation of sphere resonance: Bessel beam example, *Journal of the Acoustical Society of America* 122 (2007) 247–252.
[25] P.L. Marston, Axial radiation force of a Bessel beam on a sphere and direction reversal of the force, *Journal of the Acoustical Society of America* 120 (2006) 3518–3524.
[26] P.L. Marston, Negative axial radiation forces on solid spheres and shells in a Bessel beam (L), *Journal of the Acoustical Society of America* 122 (2007) 3162–3165.
[27] D. McGloin, K. Dholakia, Bessel beams: diffraction in a new light, *Contemporary Physics* 46 (2005) 15–28.
[28] F.G. Mitri, Langevin acoustic radiation force of a high-order Bessel beam on a rigid sphere, *IEEE Transactions on Ultrasonics Ferroelectrics and Frequency Control* 56 (2009) 1059–1064.
[29] F.G. Mitri, Acoustic radiation force on an air bubble and soft fluid spheres in ideal liquids: Example of a high-order Bessel beam of quasi-standing waves, *European Physical Journal E* 28 (2009) 469–478.
[30] F.G. Mitri, Negative axial radiation force on a fluid and elastic spheres illuminated by a high-order Bessel beam of progressive waves, *Journal of Physics A—Mathematical and Theoretical* 42 (2009) 245202.
[31] P.L. Marston, Radiation force of a helicoidal Bessel beam on a sphere, *Journal of the Acoustical Society of America* 125 (2009) 3539–3547.
[32] F.G. Mitri, Acoustic radiation force of high-order Bessel beam standing wave tweezers on a rigid sphere, *Ultrasonics* 49 (2009) 794–798.
[33] F.G. Mitri, Z.E.A. Fellah, New expressions for the radiation force function of spherical targets in stationary and quasi-stationary waves, *Archive of Applied Mechanics* 77 (2007) 1–9.
[34] V.M. Ayres, G.C. Gaunaurd, Acoustic resonance scattering by viscoelastic objects, *Journal of the Acoustical Society of America* 81 (1987) 301–311.
[35] F.G. Mitri, Acoustic scattering of a high-order Bessel beam by an elastic sphere, *Annals of Physics* 323 (2008) 2840–2850.
[36] P.L. Marston, Scattering of a Bessel beam by a sphere: II. Helicoidal case and spherical shell example, *Journal of the Acoustical Society of America* 124 (2008) 2905–2910.
[37] F.G. Mitri, Equivalence of expressions for the acoustic scattering of a progressive high-order Bessel beam by an elastic sphere, *IEEE Transactions on Ultrasonics Ferroelectrics and Frequency Control* 56 (2009) 1100–1103.
[38] B.T. Hefner, P.L. Marston, An acoustical helicoidal wave transducer with applications for the alignment of ultrasonic and underwater systems, *Journal of the Acoustical Society of America* 106 (1999) 3313–3316.
[39] T. Hasegawa, Acoustic radiation force on a sphere in a quasistationary wave field-theory, *Journal of the Acoustical Society of America* 65 (1979) 32–40.
[40] N.N. Knyaz'kov, V.E. Kurochkin, B.P. Sharfarets, Radiation pressure on a sphere in a combined field of traveling and standing plane waves, *Doklady Physics* 54 (2009) 59–62.
[41] T. Hasegawa, Comparison of two solutions for acoustic radiation pressure on a sphere, *Journal of the Acoustical Society of America* 61 (1977) 1445–1448.